Reprinted with permission from: Zhang J, Muirhead B, Dodd M, Liu L, Xu F, Mangiacotte N, Hoare T, Sheardown H An Injectable Hydrogel Prepared Using a PEG/Vitamin E Copolymer Facilitating Aqueous-Driven Gelation. Biomacromolecules 2016, 17, 3648−3658
DOI: 10.1021/acs.biomac.6b01148

Note: Some symbols and text may have become corrupted during export (e.g. μ exports to m). Please contact the corresponding author for clarification.

An Injectable Hydrogel Prepared Using a PEG/Vitamin E Copolymer Facilitating Aqueous-Driven Gelation

Jianfeng Zhang,[†] Ben Muirhead,[‡] Megan Dodd,[†] Lina Liu,[†] Fei Xu,[†] Nicole Mangiacotte,[†] Todd Hoare,[†,‡] and Heather Sheardown*[,†,‡]

[†]Department of Chemical Engineering, [‡]School of Biomedical Engineering, McMaster University, Hamilton Ontario L8S 4L7, Canada

ABSTRACT: Hydrogels have been widely explored for biomedical applications, with injectable hydrogels being of particular interest for their ability to precisely deliver drugs and cells to targets. Although these hydrogels have demonstrated satisfactory properties in many cases, challenges still remain for commercialization. In this paper, we describe a simple injectable hydrogel based on poly(ethylene glycol) (PEG) and a vitamin E (Ve) methacrylate copolymer prepared via simple free radical polymerization and delivered in a solution of low molecular weight PEG and Ve as the solvent instead of water. The hydrogel formed immediately in an aqueous environment with a controllable gelation time. The driving force for gelation is attributed to the self-assembly of hydrophobic Ve residues upon exposure to water to form a physically cross-linked polymer network via polymer chain rearrangement and subsequent phase separation, a spontaneous process with water uptake. The hydrogels can be customized to give the desired water content, mechanical strength, and drug release kinetics simply by formulating the PEGMA-co-Ve polymer with an appropriate solvent mixture or by varying the molecular weight of the polymer. The hydrogels exhibited no significant cytotoxicity in vitro using fibroblasts and good tissue compatibility in the eye and when injected subcutaneously. These polymers thus have the potential to be used in a variety of applications where injection of a drug or cell containing depot would be desirable.

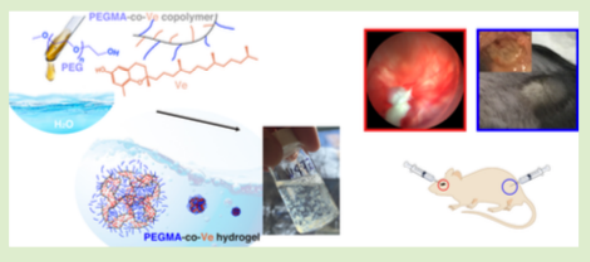

INTRODUCTION

Hydrogels are physically or chemically cross-linked polymeric networks that are capable of retaining large amounts of water or biological fluids[1,2] and have been extensively explored for cell and drug delivery in a variety of applications.[3,4] Conventionally, hydrogels utilized as biomaterials are prepared ex vivo and surgically implanted at their site of action. Given the invasiveness of this approach, there has been a great deal of interest in the development of hydrogel materials that can be injected as a liquid and then gel in situ.[4–7] Such in situ gelling injectable hydrogels have significant benefits in terms of practical clinical applicability, as these materials have the potential to allow for precise delivery of cells or drug without invasive surgery, reducing the risk of infection, minimizing trauma to the surrounding tissue and organs, and alleviating pain.[7,8]

As suggested by the name, for a hydrogel to be injectable, precursors should be in liquid form, preferentially with low viscosity. Furthermore, practically, the solid hydrogel should be formed rapidly following injection into the target tissue, allowing the hydrogel to act as a drug or cell depot that can slowly release its payload.[4,8] The challenge of making a practical injectable hydrogel delivery system is thus to design a polymer solution that can respond to environmental stimuli and/or form covalent bonds upon injection rapidly and with controllable gelation kinetics without creating back-pressure at the site of injection.[8] In general, in situ gelation is driven either by chemical reaction or physical interaction.[7,9] Chemical crosslinking can occur by such mechanisms as click chemistry,[8,10–12] disulfide-cross-linking,[13] Michael addition,[14–16] and photocross-linking,[17–19] among other reactions.[7,20–22] For most chemically cross-linked hydrogels, regardless of the biocompatibility of the polymers used, concerns often still remain regarding the potential toxicity of any residual reactive functional groups as well as the potential for side reactions with biomacromolecules in vivo with many commonly used chemistries.[23,24] Alternatively, polymeric hydrogels can physically cross-link upon exposure to stimuli from the environment such as temperature and pH.[7,11,25–34] Although these stimuli sensitive hydrogels are believed to be less toxic,[24] deficiencies remain. Specifically, depending on the formulation, controlling the gelation rate,[34] the mechanics,[11] and the degradation[35,36] of such hydrogels can be highly challenging,

particularly while avoiding the use of very high polymer concentrations.[37] Thus, there are only a few hydrogels available that have been Flamel's Medusa).[38–40]

For expediency in pharmaceutical applications, FDA approved chemical compounds are the best candidates for use in polymer design.[32] Poly(ethylene glycol) (PEG) is an FDA-approved and commercially available synthetic polymer that has been widely used in medical applications for its low cytotoxicity, low immunogenicity, and protein repellent properties.[8,41] Vitamin E (Ve) plays an important role as a factor for scavenging free radicals, as well as acting as an antiinflammatory and an antithrombolytic.[42–44] Ve and its derivatives (e.g., TPGS, vitamin E polyethylene glycolsuccinate) have been used in drug delivery applications due to their capacity to solubilize various hydrophobic drugs and their often synergistic enhancement to the delivery efficiency.[45–47]

In this paper, we describe a simple injectable hydrogel based on PEG and Ve. The PEGMA-co-Ve polymer was synthesized under mild conditions via free radical polymerization of PEG methacrylate and methacrylated Ve. By using low molecular weight PEG with Ve as the solvent instead of using water (a "solvent" system particularly effective for loading hydrophobic drugs), gelation can be triggered by the presence of water over a wide range of temperature and pH. The driving force for gelation is attributed to water-induced polymer chain rearrangement and self-association of hydrophobic Ve segments to form physical cross-links, a process that occurs spontaneously upon water uptake by the hydrogel precursor; to the best of our knowledge, such a process has not yet been reported as a mechanism for in situ gelation. We demonstrate this aqueousdriven gelation process occurs consistently both in vitro and in vivo, and that the gelation time can be tuned by altering the molecular weight of copolymer, and weight ratio of Ve used as "solvent". Also, these hydrogels have customizable water contents, mechanical strengths, and drug release kinetics facilitated simply through formulating the PEGMA-co-Ve polymer with different solvent (Ve and PEG) combinations or varying the molecular weight of the polymer. Cytocompatibility and in vivo tissue compatibility also indicated high tolerability of the formulations in multiple biological environments, suggesting the potential for using this approach for the formation of practical in situ-gelling materials.

EXPERIMENTAL SECTION

Materials. Vitamin E ((+)-δ-Tocopherol), poly(ethylene glycol) methyl ether methyl acrylate (PEGMA, M_w ~ 960 g/mol), poly(ethylene glycol) (PEG, Mw ~ 300 g/mol), methacryloyl chloride, benzoyl peroxide (BPO), inhibitor remover, methylthiazolyldiphenyl-tetrazolium bromide (MTT reagent), calcein AM, ethidum homodimer-1, atropine, and atropine sulfate salt monohydrate were purchased from Sigma-Aldrich. All solvents were purchased from Caledon Laboratories and used as received.

Chemistry. Synthesis of Methacrylated Vitamin E. A methacrylated Ve monomer was synthesized from methacryloyl chloride (0.324 g, 3.13 mmol, 1.25 equiv) and Ve (1 g, 2.5 mmol, 1 equiv). The methacrylol chloride was added dropwise into Ve in a tetrahydrofuran (THF, 15 mL) and triethylamine, (0.632 g, 6.26 mmol, 3 equiv) solution. The reaction was performed under nitrogen and was initially kept in a 0 °C ice bath for 4 h followed by room temperature for additional 18 h. After the reaction, the resultant salt (triethylamine hydrochloride) was removed by filtration. The solvent was then evaporated to give the crude methacrylated Ve monomer. This crude product was redissolved in anhydrous THF (5 mL) to precipitate any salt residues, with the process repeated once more for purification. Of additional note, there was methacrylic acid existing as by product due to moisture; and it could be removed by running through a silica column. Finally, the product was left in a vacuum oven at room temperature for 12 h. The methacrylated Ve monomer was stored under nitrogen and away from light.

Copolymerization of Methacrylated Vitamin E and PEG Methacrylate. For the synthesis of PEGMA-co-Ve, methacrylated Ve, PEGMA, and BPO were dissolved in 1,4-dioxane. The solution was first purged with nitrogen for 5 min, after which the reaction vessel was sealed and placed into an 80 °C oil bath for 24 h. The molecular weight of PEGMA-co-Ve could be adjusted by simply varying the amount of initiator (Table 1). After the reaction, the solution was first cooled to room temperature and then added dropwise to cold ether (ca. –20 °C, 100 mL) under stirring to precipitate and collect PEGMA-co-Ve polymer. This purification was repeated once. Finally, the residual solvent in the polymer was removed in a vacuum oven (40 °C, 12 h).

Table 1. Synthesis Recipes for PEGMA-co-Ve Polymer

	reagents				GPC			
PEGMA-*co*-Ve[a]	PEGMA (g)	methacrylated Ve (g)	BPO (mg)	1,4-dioxane (mL)	M_n (g/mol)	M_w (g/mol)	M_z (g/mol)	dispersity (Đ)
# 20	2	1	37	20	15 500	32 500	48 000	2.10
# 50	2	1	14.8	20	24 000	54 500	83 500	2.26
# 100	2	1	7.4	20	23 000	60 000	113 500	2.59

[a]The numbers represent the nominal/targeted molecular weight of PEGMA-*co*-Ve.

Formulation of Injectable Hydrogel Precursor. The PEGMAco-Ve polymer was formulated with low molecular weight (~300 Da) PEG and Ve to generate the injectable hydrogel precursor solution (Table 2). PEGMA-co-Ve polymer, PEG, and Ve were placed in a vial and heated up to 80 °C until the polymer was melted and miscible with PEG and Ve. The precursor was mixed by hand, resulting in a brown but transparent mixture ready for injection either into water or tissue.

Table 2. Formulations of PEGMA-co-Ve Injectable Hydrogel Precursor Solutions

	PEGMA-*co*-Ve				
sample code[a]	#	mass (g)	PEG (g)[b]	Ve (g)	water content (% of original mass)[c]
$20P_{43\%}PEG_{57\%}Ve_{0\%}$	20	0.15	0.2	-	-[d]
$20P_{33\%}PEG_{45\%}Ve_{22\%}$	20	0.15	0.2	0.1	400
$50P_{33\%}PEG_{45\%}Ve_{22\%}$	50	0.15	0.2	0.1	260
$50P_{42\%}PEG_{29\%}Ve_{29\%}$	50	0.15	0.1	0.1	130
$50P_{60\%}PEG_{0\%}Ve_{40\%}$	50	0.15	0	0.1	120
$100P_{33\%}PEG_{45\%}Ve_{22\%}$	100	0.15	0.2	0.1	-[e]

[a]The sample was code in the form $\#\#P_{\#\#\%}PEG_{\#\#\%}Ve_{\#\#\%}$, in which the first number is the nominal/targeted molecular weight of PEGMA-*co*-Ve polymer (e.g., 20 = 20 000 g/mol) and subscripts refer to the weight percentage of PEGMA-*co*-Ve, PEG, and Ve in the formulation, respectively. [b]The molecular weight of PEG used as solvent is 300 g/mol. [c]The water content is calculated via gravimetry 12 h following injection of the precursor solutions into water, using the formula % Water = $Mass_{water}/(Mass_{PEGMA\text{-}co\text{-}Ve} + Mass_{PEG} + Mass_{Ve}) \times 100\%$. [d]This mixture formed micelles instead of a bulk gel, and thus no measurement is reported for the water content or the modulus. [e]This formulation was not a viable injectable hydrogel precursor due to the high molecular weight and thus the viscosity of PEGMA-*co*-Ve.

Characterization. NMR spectra for methacrylated Ve monomer and PEGMA-co-Ve polymer were recorded on a Bruker Avance 600 MHz nuclear magnetic resonance spectrometer using deuterated chloroform as the solvent. Spectra were used to determine the ratio of PEG to Ve in the copolymer.

The molecular weight of PEGMA-co-Ve copolymers was characterized by a Polymer Laboratories PL-50 GPC (gel permeation chromatograph) using N,N-dimethylformamide (DMF) with 50 mM LiBr as the solvent. The GPC was equipped with three Phenomenex Phenogel columns (300 × 4.6 mm, 5 μm; pore sizes: 100, 500, 10^4 Å). The elution rate was set at a 0.3 mL/min. The system was calibrated with PEG standards with molecular weights ranging from 600 to 167 000 g/mol. All samples were filtered using a 0.2 μm Teflon filter.

The morphologies of hydrogels were examined using scanning electron microscopy (SEM). Hydrogel samples were freeze-dried and then extracted with cold ether twice at −20 °C for 24 h, after which the dried hydrogels were left in a vacuum oven for 2 h. Samples were coated with a 10 nm coating of gold prior to imaging.

The mechanical performance of hydrogels immersed in water was tested using a MicroSquisher (CellScale Biomaterials Testing, Waterloo, Canada) under compression mode. The cantilevers were fabricated using a 558.8 μm gauge cantilever and a square platen. During the test, a displacement of 20% was applied per compression. The durations of loading and recovery were 20 and 40 s, respectively. The compression modulus of a bulk hydrogel (sample thickness = 2.43 mm, diameter = 12.5 mm) was measured with an ARES rheometer (Texas Instruments) operating under parallel-plate geometry with a 20% displacement, as the comparison to MicroSquisher.

The water content of hydrogel was determined by measuring the weight of gel saturated with water relative to the weight of gel after drying in a 100 °C oven.

Cytotoxicity of PEGMA-co-Ve, PEG, and Ve. Murine 3T3 fibroblasts were seeded in 96-well plates at a density of 8000 cells per well and cultivated in 100 μL of DMEM growth medium at

37 °C for 4 h to reach ~50% confluency. Growth medium was then replaced with 100 μL of fresh medium together with PEG (3% of the medium volume), Ve (3% of the medium volume), and PEGMA-co-Ve (~10 mg polymer). Each condition was tested in triplicate. Following a 48 h incubation under standard culture conditions (37 °C and 5% CO_2), the culture medium was replaced with 100 μL Fluorobrite media and 10 μL MTT reagent and incubated at 37 °C for an additional 3 h. The Fluorobrite-MTT solution was then removed, and 50 μL DMSO was added to dissolve the internalized purple formazan crystals. The absorbance of metabolized products was read using a microplate reader (Infinite M200 Pro, Tecan) at 540 nm. Viability results were expressed as a percentage of the absorbance of the control cells without any treatment.

For the live/dead staining, cells were plated and treated as described for the MTT assay. Following a 48 h incubation, the cells were observed and culture media removed. Cells were washed gently with 100 μL of phosphate buffered saline (PBS) to remove any residual media and samples, and 50 μL PBS was added to each well. To three control wells, 100 μL of 70% ethanol was added to prepare a dead control. Fluorescent stain solution was prepared at 2 μM calcein AM and 4 μM ethidium homodimer-1 (EthD-1) in PBS, after which 50 μL of each stain was added to each well. Control wells (containing either live or dead cells) were also treated with both calcein AM and EthD-1 or calcein AM and EthD-1 alone. Following a 30 min incubation under dark conditions, cells were photographed using the Axiovert 200 fluorescent microscope (Zeiss) and assessed using AxioVision microscopy software.

In Vitro Release of Atropine and Atropine Sulfate. To examine the potential of the PEGMA-co-Ve hydrogels to deliver drugs, atropine and atropine sulfate were used given their potential application in the eye. Given that atropine can be dissolved in Ve, it was added directly to the soluble Ve fraction to form a homogeneous solution before formulating the injectable hydrogel precursor; by contrast, atropine sulfate can only be dispersed in Ve such that it was added after formulating the precursor (to avoid potential issues with the solubility of PEGMA-co-Ve in Ve with atropine sulfate premixed). The final formulations of hydrogel precursors and loaded drug are shown in Table 3. The drug release tests were performed using a FloatA-Lyzer G2 Dialysis Device (MW cut off: 300 kDa) using an inverse geometry, in which the drug-containing gel was located outside the membrane and the replaced (sampling) buffer is inside the membrane (Figure S1, Supporting Information). For $50P_{33\%}PEG_{45\%}Ve_{22\%}$/ Atropine, 76.4 mg of hydrogel precursor (containing ~5 mg Atropine) was injected into a device containing 6 mL Milli-Q water; an analogous procedure was used to prepare $50P_{42\%}PEG_{29\%}Ve_{29\%}$/ Atropine (66.5 mg gel precursor, ~ 5 mg Atropine) and $50P_{33\%}PEG_{45\%}Ve_{22\%}$/Atropine sulfate (165.7 mg gel precursor, ~ 10 mg Atropine sulfate). At predefined time points, 1 mL of solution was sampled from inside the dialysis bag to monitor drug release, followed by refilling with Milli-Q water to maintain a fixed overall volume in the devices at all times. The devices were kept under shaking (circulating in horizontal plane, 60 rpm) and sampled at following intervals: 10 min, 30 min, 1 h, 3 h, 6 h, 12 h, 24 h, 48 h, 73 h, 100 h, 1 week, 2 weeks, and 3 weeks. The amount of drug released was quantified using high-performance liquid chromatography (HPLC, Waters, detecting UV absorption at 254 nm and using an Atlantis dC18 5 μm 4.6 × 100 mm column, solvent: mixture of 60/40 water/acetonitrile, flow rate: 1 mL/min). The data were obtained based on a single experiment for each formulation.

Table 3. Formulation of Injectable Hydrogel Precursors for *in Vitro* Drug Release

formulation	PEGMA-*co*-Ve (#50, g)	PEG (g)	Ve (g)	atropine (g)	atropine sulfate (g)
$50P_{42\%}PEG_{29\%}Ve_{29\%}$/ Atropine	0.15	0.1	0.1	0.03	-
$50P_{33\%}PEG_{45\%}Ve_{22\%}$/ Atropine	0.15	0.2	0.1	0.03	-
$50P_{33\%}PEG_{45\%}Ve_{22\%}$/ Atropine sulfate	0.15	0.2	0.1	-	0.03

In vivo Injections and Histology Analysis. To examine the in vivo toxicity of the materials, Sprague–Dawley rats (strain code 400) and C57BL/6 mice (strain code 27) were used. All animals were handled according to the principles of the ARVO Statement for the Use of Animals in Vision Research as well as the guidelines set out by McMaster AREB and the Canadian Council of Animal Care. The eye was chosen as an injection target as it represents an ideal location to observe gelation kinetics in vivo, and such materials have the potential to deliver drugs for the treatment of various eye conditions. Male Sprague–Dawley rats (~500 g) were injected with 10 to 50 μL of sterile material precursor into the vitreous using a 10-μL 700 series Hamilton syringe and a 30 gauge needle. Animals were induced with isofluorane and anaesthetized with a ketamine xylazine mixture.

The injection and in situ gelation process was monitored and recorded using a dissecting microscope and the Micron IV fundus camera (Phoenix Research Laboratories). The rats were sacrificed 4 h after injection, after which the eyes were enucleated. The eye samples were fixed in 4% neutral buffered formalin (NBF) for 24 h, followed by standard histological processing and embedding into paraffin wax. Whole eyes were processed into 5 μm sections along the sagittal plane. Tissue samples were stained using hematoxylin and eosin (H&E) following standard protocols, with the resulting cross sections examined using a conventional light microscope (Olympus, BX51).

The long-term fate of these hydrogel materials was also studied via a subcutaneous injection study. Male mice (~25 g) were injected with 100 μL of $50P_{42\%}PEG_{29\%}Ve_{29\%}$ precursor solution subcutaneously in the flank using a 25 gauge syringe. After 15 days, mice were sacrificed and the injection site was explanted. Both cryosectioning and conventional paraffin histology were performed in an attempt to preserve the hydrogel, which is miscible in the organic solvents needed with wax. In either case, samples were fixed in 4% NBF as above for 24 h, cleared in ethanol, then either processed for paraffin embedding or snap-frozen in optimal cutting temperature (OCT) compound in a bath of isopentane cooled by liquid nitrogen. Sections were created using a microtome or cryostat as required and stained with H&E as above

RESULTS AND DISCUSSION

Synthesis of Methacrylated Ve and PEGMA-co-Ve Polymer. The synthesis of methyl acrylated Ve monomer and PEGMA-co-Ve polymer are both straightforward, with each requiring only a two-step synthesis using commercially available products (Figure 1).

Preparation of the methacrylated Ve monomer proceeded via a condensation reaction at high yield (>90% conversion). PEGMA-co-Ve polymer was prepared via thermally initiated free radical polymerization, which also proceeded to a high yield (~90%, after repeated purification in cold ether). Both the ^{1}H NMR and ^{13}C NMR confirmed that PEGMA and methacrylated Ve successfully copolymerized (Figure S3, Supporting Information). Results demonstrate that polymer molecular weight control can be achieved by adjusting the molar ratio of the initiator to the monomers (Table 1), although as the amount of initiator decreases (e.g., between #50 and #100), the relative values of M_z versus M_n suggest that the large chains become significantly larger when initiator is reduced without significantly shifting the number-average polymer size distribution. The molecular weights characterized using GPC did not exactly match the targets (not surprised for normal free radical polymerization); however, given the use of linear PEG as a calibration standard, such deviations are expected given the significant difference in both structure (PEG is a linear polymer while PEGMA is a comb-like polymer) and solvation (based both on the different backbones and the presence of Ve segments) between the PEGMA-co-Ve and the PEG calibration standard. The monomer ratio (PEG/Ve) in the polymer was roughly reflected in the ratio of the monomers in the reaction mixture; however, the ratio of PEG to Ve in copolymer increased from 1.27 to 1.67 with increasing molecular weight despite the feed ratio of PEG to Ve being fixed at 1:1 (Figure 1, and Figure S3, Supporting Information), suggesting that PEGMA was somewhat more kinetically reactive than Ve. Not unexpectedly for standard free radical copolymerization, the PEGMA-co-Ve polymers were found to have a large polydispersity index (PDI > 2, Table 1). However, it is believed that this high PDI may actually help to facilitate aqueous-driven gelation, providing a mixture of lower molecular weight polymer (with potential for faster reorientation in water and thus faster gelation) and high molecular weight polymers (providing structural support for the resulting gel). The use of simple free radical polymerization requires less demanding conditions (i.e., lower sensitivity to oxygen, and insensitivity to water) than controlled free radical techniques such as RAFT (reversible addition–fragmentation chain transfer) and ATRP (atom transfer radical polymerization), making it easier to scale up this polymerization for commercial production.

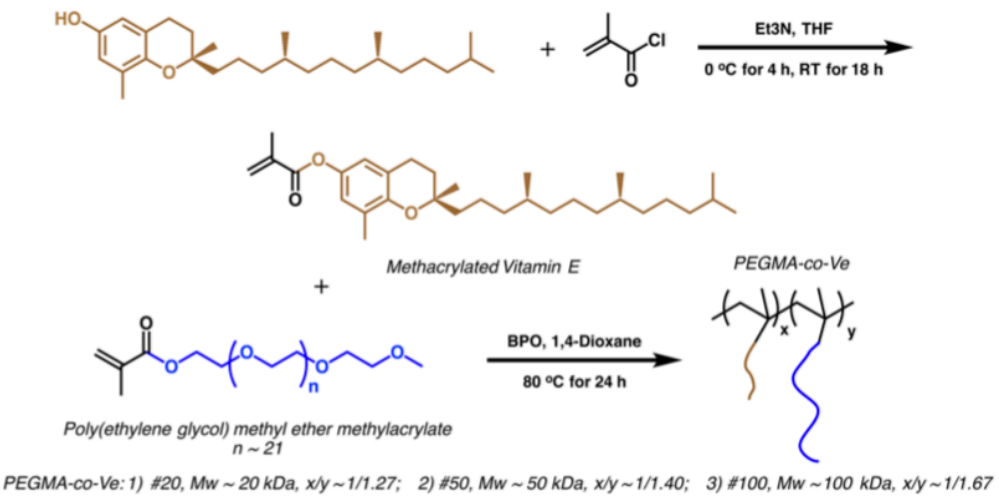

Figure 1. Synthesis of methacrylated Ve monomer and subsequent free radical polymerization to produce PEGMA-*co*-Ve copolymer.

Aqueous-Driven Gelation in Water and Tissue. The gelation of hydrogel precursor can be driven by a variety of mechanisms including chemical cross-linking or physical crosslinking caused by changes in polymer hydrophobicity.[7,9] Conventional physical hydrogels cross-linked via hydrophobic interactions are delivered in vivo in aqueous solvents, with either the shear thinning capacity of the hydrophobic interactions used to temporarily reduce the viscosity and enable injection or a phase transition triggered by the physiological environment creating hydrophobically associating groups specifically in the body.[4–7] By contrast, aqueous-driven gelation of PEGMA-co-Ve polymers is hypothesized to proceed via a solvent exchange mechanism, as schematically illustrated in Figure 2A. In our injectable hydrogel precursor, low molecular weight PEG and Ve were used as solvents instead of water to dissolve PEGMA-co-Ve and the drug, creating a solution with minimal driving forces for phase separation. However, upon exposure to water, the presence of the PEG solvent in addition to the PEG blocks provide a significant osmotic driving force for water uptake, accompanied by reorientation of the PEG-rich domains in the polymer to the interface and transport of the highly soluble PEG solvent out of the polymer network. Water intake then drives hydrophobic phase separation of both the added Ve as well as the Ve blocks on the polymer, forming domains within the PEG-based gel phase that serve as physical cross-linking points (i.e., Ve grafts anchored by soluble Ve). The gelation process is completed once the osmotic pressure inside and outside of the hydrogel reaches equilibrium, as determined by the amount and mobility of PEG as well as the amount of free Ve and the density of Ve groups grafted to the polymer. As a comparison, blends of PEG and Ve monomers (without the two components being copolymerized together as in PEGMA-co-Ve) fully phase separated in water, forming neither a gel nor a stable emulsion.

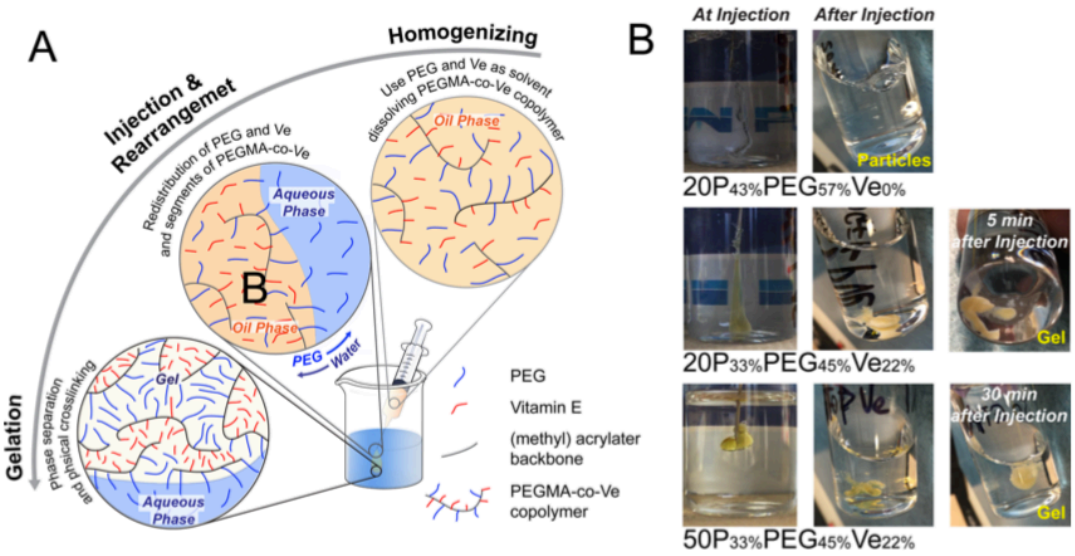

Figure 2. (A) Schematic illustration of aqueous-driven gelation of PEGMA-*co*-Ve in water, and (B) injection of hydrogel precursors with different compositions into water.

The components of the precursor solution are critical not only for affecting the aqueous-driven gelation process, but also for giving the hydrogel appropriate physical properties including the targeted water contents, mechanical properties, degradation times, and drug release kinetics.

Gelation Time. In the hydrogel precursor solution, PEG and Ve serve not only as a solvent for PEGMA-co-Ve but also as osmotic and phase separation materials that directly regulate both the speed and extent of gelation. As shown in Figure 2B to D, the precursors could transform to particles in suspension or to a gel with the variation of composition. Ve is a critical component to this gelation process; as shown in Figure 2B, $20P_{43\%}PEG_{57\%}Ve_{0\%}$ (containing PEG and PEGMA-co-Ve but no added Ve) formed suspended particles immediately upon injection in water instead of a gel, suggesting that there is insufficient hydrophobic content in the precursor solution to form the larger hydrophobic domains required for gel formation (resulting instead in self-assembly of PEGMA-coVe to form polymeric micelles dispersed in the aqueous phase). Upon addition of Ve, the precursors were able to gel in situ as shown in Figure 2C and D, with complete gelation observed over times ranging from 5 min (lower polymer molecular weight) to 30 min (higher polymer molecular weight). The gelation time is mainly determined by factors including the composition of the formulation, the molecular weight of the PEGMA-co-Ve (related here primarily to differences in polymer chain mobility), and the volume of the precursor solution exposed to water. Given that water diffusion is essential for gelation, unlike most injectable hydrogel formulations, smaller volumes will gel more quickly; of particular consequence in this study, faster gelation in vivo is expected due to the significantly lower sample volumes injected compared to the in vitro study (~1 min required for gelation in eye, video in the Supporting Information; compared at 5 min in water in the in vitro study, Figure 2C). Of additional note, if the Ve

monomer was also purified via a silica gel after preparation to remove possible methacrylic acid byproduct, and subsequently used to remake polymer #50; identical gelation process occurred, as shown in Figure 2B, indicating this gelation process was mainly governed by the rearrangement of PEG and Ve blocks.

Water Content, Morphology, and Mechanical Performance. The physical properties of hydrogel are easily controlled through adjustments to the formulation. As shown in Table 2, the water content in the gels decreased with a reduction in the amount of low molecular weight PEG solvent in the precursor solutions, consistent with an osmotically driven mechanism of gelation. Furthermore, increasing the molecular weight of the PEGMA-co-Ve polymer reduced the water uptake over the first 12 h, consistent with the observed slower gelation times with higher molecular weight formulations; this result can be attributed to the higher viscosity and potential for higher hydrophobic cross-link formation with such precursor polymers that would limit the swelling of the gels over time. Due to the importance of water content on drug release from the hydrogel,[7,48] the capacity to alter this parameter directly by choice of solvent and/or choice of polymer facilitates flexibility in adapting the materials to different applications.

While it is recognized that SEM on lyophilized hydrogels does not give direct information on the pore size in the hydrated state, SEM can give some insight into the relative nature of the gelation process associated the chain rearrangement and phase separation of PEG and Ve.[49−51] As shown in Figure 3, the porosity of the gel decreased with the fraction of "solvent" (i.e., low molecular weight PEG and Ve) in the precursor solution as well as the water content of the resulting gel, with water content giving the clearest impact on gel morphology. For example, while the fraction of solvent (PEG and Ve) only decreased by ~10% moving from $50P_{33\%}PEG_{45\%}Ve_{22\%}$ to $50P_{42\%}PEG_{29\%}Ve_{29\%}$ (Table 2), the water content was reduced by ~100% (Table 2) and a marked increase in apparent gel density was observed in the SEM images (Figure 3B,C). By contrast, bead-like structures were prepared in the gel using Ve only as solvent (Figure 3D). The gel network structure was also impacted by the molecular weight of PEGMA-co-Ve. Gels presented as primarily fibrous in morphology when a lower molecular weight polymer was used (Figure 3A), while bicontinuous or twisted structures were primarily observed with higher molecular weight polymer (Figure 3B–D).

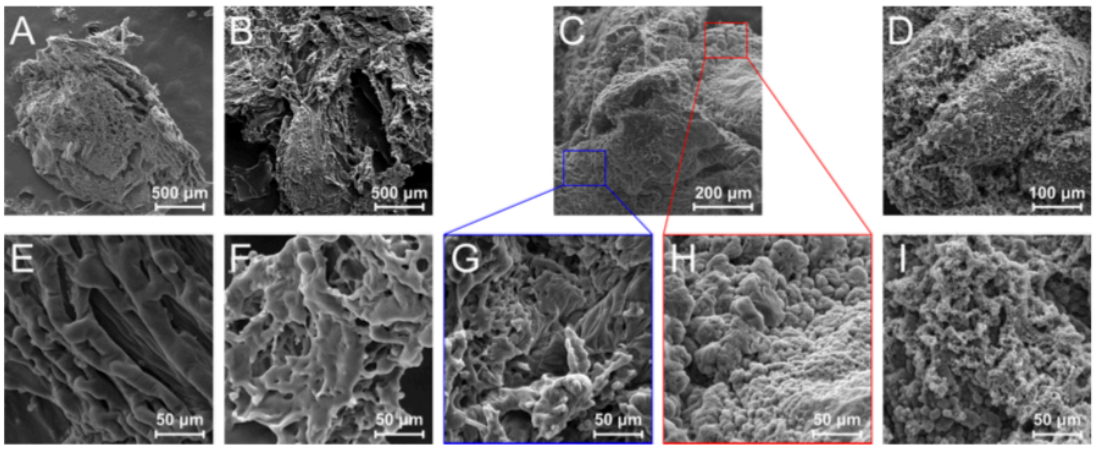

Figure 3. SEM images of hydrogel morphologies after freeze-drying and extraction of Ve and low molecular weight PEG. (A) 100× and (E) 1000× magnification of $20P_{33\%}PEG_{45\%}Ve_{22\%}$ gel; (B) 100× and (F) 1000× magnification of $50P_{33\%}PEG_{45\%}Ve_{22\%}$ gel; (C) 300× and (G, H) 1000× magnification of $50P_{42\%}PEG_{29\%}Ve_{29\%}$ gel; (D) 500× and (I) 1000× magnification of $50P_{60\%}PEG_{0\%}Ve_{40\%}$ gel.

Control over hydrogel morphology and water content is expected to result in significantly different mechanical performance of the hydrogels. Ideally, the mechanics of the gels should mimic that of the tissue at the injection site.[52,53] The hydrogels prepared covered a wide range of moduli varying between 0.005 to 3.5 kPa, (Table 4 and Figures S4 and S5, Supporting Information), with higher stiffness achieved by using a higher content of PEGMA-co-Ve, a higher amount of Ve, and/or a higher molecular weight of PEGMA-co-Ve in the formulation. The compression modulus of $50P_{60\%}PEG_{0\%}Ve_{40\%}$, the strongest gel in this series, demonstrated values in the same order of magnitude, when using the MicroSquisher and the rheometer as the characterization method (~3.5 kPa from MicroSquisher, and ~1.1 kPa from rheometer, respectively, Figures S4 and S5).

Table 4. Mechanical Performance of PEGMA-co-Ve Hydrogels

	modulus (Pa)		stress reduction (%)[a]			plastic deformation (%)[b]		
sample code	initial	final	2nd cycle	final cycle	standard deviation[c]	2nd cycle	final cycle	standard deviation
$20P_{33\%}PEG_{45\%}Ve_{22\%}$	~5	~5	5	52	21	0	~6	3
$50P_{33\%}PEG_{45\%}Ve_{22\%}$	~16	~10	0	43	20	~0	~0	-
$50P_{42\%}PEG_{29\%}Ve_{29\%}$	~100	~100	12	24	6	2.5	~4	<0.5
$50P_{60\%}PEG_{0\%}Ve_{40\%}$	~3500	~2000	4	32	21	1.5	8	3

[a]The stress reduction describes the percentage decrease of peak stress relative to the initial stress, e.g., stress reduction of last cycle % = (peak stress at last cycle−initial peak stress)/initial peak stress ×100%. [b]The plastic deformation is defined as the irreversible deformation after a given number of cycles, as read at the intersection of tensile curve at 0 stress (see Figure S4 for details). [c]The standard deviation of the stress reduction percentage over 20 ($20P_{33\%}PEG_{45\%}Ve_{22\%}$) or 30 times (rest samples) compression cycles.

As shown in Figure S4 and Table 2, hydrogels made from $50P_{42\%}PEG_{29\%}Ve_{29\%}$ demonstrated the most reversible mechanics over 30 cycles following a small amount of hysteresis after cycle one. Either too weak ($20P_{33\%}PEG_{45\%}Ve_{22\%}$) or too stiff hydrogels ($50P_{60\%}PEG_{0\%}Ve_{40\%}$) experienced more irreversible deformation with continuous application of external force, ranging ~0% up to 8% after 30 cycles depending on the formulations (Table 4 and Figure S4). Thus, the viscoelastic response of the hydrogels was customizable for potential applications in a variety of tissue types.

Degradation and Drug Release. As the hydrogels were designed to serve as drug depots, the decomposition of the hydrogels is a critical parameter in their application. Hydrogels prepared from $50P_{33\%}PEG_{45\%}Ve_{22\%}$ slowly fractured and degraded over a two months period (Figure S6, Supporting Information). These gels first fractured into many small pieces after 10 days of shaking under mild conditions (~120 rpm, 37 °C, Figure S6); beyond day 30, a significant number of particles was observed with sizes ranging between 100 and 800 nm (Figure S7, Supporting Information), with the hydrogel fully visually degraded after two months. This degradation mechanism is consistent with the gradual leaching of both PEG and Ve from the matrix driving reduced gelation and increasing micellization over time in this polymer, consistent with the observed micellization in formulations initially prepared without Ve (Table 2). The period of this "degradation" was controllable based on the degree of hydration of the hydrogels; for example, hydrogels prepared from $20P_{33\%}PEG_{45\%}Ve_{22\%}$ that exhibited significantly higher water uptake were visually degraded in just 20 days (Figure S8, Supporting Information). As such, the rate of gel degradation is mainly determined by water content, with higher water content gels dispersing much more rapidly than lower water content gels.

Although the hydrogel was demonstrated to disperse over time, the hydrogel must also be degradable and excreted from the body for practical in vivo use.[54] In our formulation, all of the components in the precursors are easily processed by the body. Vitamin E can be taken up and metabolized; the low molecular weight PEG can be easily cleared through the kidney (threshold: 20–60 kDa).[55,56] The PEGMA-co-Ve polymer, depending on its molecular weight, could be either excreted through kidney or degraded to low molecular weight fractions before excretion. It has been demonstrated that an ester bond such as those linking the PEG side chains and Ve to the polymer backbone can be hydrolyzed under physiological conditions,[57] leaving a water-soluble polymer poly(methacrylic acid) degradation product with a molecular weight below kidney threshold (M_w = 2.4–12 kDa).

Drug release kinetics of a hydrophobic (atropine) and a hydrophilic (atropine sulfate) drug from the resulting gels were subsequently assessed. The drug loading (by mass) was 6.7%, 8.6%, and 6.7% for $50P_{33\%}PEG_{45\%}Ve_{22\%}$/Atropine, $50P_{42\%}PEG_{29\%}Ve_{29\%}$/Atropine, and $50P_{33\%}PEG_{45\%}Ve_{22\%}$/Atropine sulfate respectively, assuming quantitative drug loading following drug entrapment inside the gel (Table 3). As shown in Figure 4, ~ 50% of loaded atropine was released from the gel within the first 3 days (73 h), followed by slow release of the remaining drug thereafter (~10% over the next 18 days). However, only ~2% of atropine sulfate was released over the first 3 days, with only an additional ~1% released over the following 18 days. Sustained release of drug was thus observed for both drugs (although to a greater extent for the hydrophilic drug), with the drug release profile mainly determined by the solubility of the drug in Ve and PEG (i.e., atropine is

fully soluble in both, while atropine sulfate is completely insoluble in both). The release of drug from the hydrogel may occur through a combination of potential mechanisms: (a) concentration gradient-driven diffusion (drug diffuses out simply because the higher concentration in gel); (b) convection-induced release (drug trapped in the gel releases with the diffusion of PEG or Ve out of the gel, or with the fragmentation of gel); (c) micellization release (drug contained in micelles diffuses out of gel as micelles are released upon bulk gel reassembling), and (d) release following gel decomposition (drug localized in the gel or micelle releases as the polymeric structure around the drug degrades, mainly due to ester hydrolysis) (Figure S6B, Supporting Information). Therefore, for a Ve-soluble drug (atropine), the release rate was initially fast due to the high concentration gradient; after 2 weeks, the release slowed down as the concentration gradient was reduced, with additional drug release occurring primarily through micellization and later decomposition of polymer (Figure S5B). As a comparison, due to the insolubility of atropine sulfate in Ve, the atropine sulfate was suspended instead of dissolved in the gel precursor and, following hydration, becomes trapped in suspension within the rapidly precipitating Ve-rich phases, forming a physical and solubilization-related barrier to impede concentration-driven diffusion. Release of the hydrophilic drug would thus be very slow, since it relies on much slower micellization and decomposition processes (as well as perhaps solubilization processes) that primarily occur outside the tested time period for this hydrogel (Figure S6C). Nevertheless, this result is highly relevant given that hydrophilic drugs are usually more difficult to deliver over prolonged periods of time.

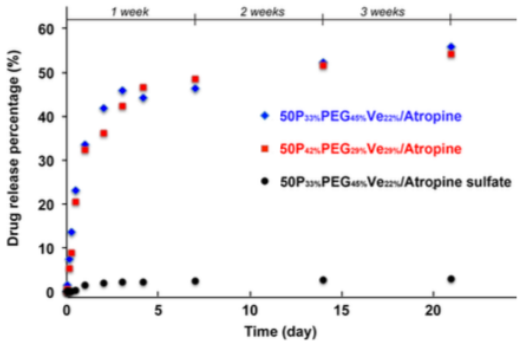

Figure 4. Drug release profiles of atropine and atropine sulfate from hydrogels over a 3-week period.

Cytotoxicity of Compositions for Injectable Hydrogel Precursor. Ideally, the hydrogels should not elicit any cytotoxic response. Therefore, in vitro compatibility was assessed using murine 3T3 fibroblasts. Figure 5 shows cell viability after treatment with low molecular weight PEG (1% v/ v to media, Figure 5C), Ve (3% v/v to media, Figure 5D), and PEGMA-co-Ve (polymer #20, #50, #100, Figure 5E to G) using both live/dead fluorescent cell labeling and MTT assay results (Figure 5H). A total of three replicate experiments were conducted per sample. Figure 5A and B represent fluorescent labeling of live and dead control cells, respectively. Live cells were labeled with calcein AM and fluoresced green, and dead cells were labeled with ethidium homodimer-1 and fluoresced

red. Although PEG and Ve are generally considered to have very low or no cellular toxicity, growth of cells neighboring hydrogels might still be affected by high local concentrations. Therefore, high doses of PEG and Ve were applied to study tolerance. For cells in media with 1% v/v low molecular weight PEG, cell viability was close to 70% of controls, indicating minimal toxicity to the fibroblasts (Figure 5H). Dead cells can detach from the surface resulting in blank regions with neither green (live) nor red (dead) cells.[58] As shown in Figure 5C, although certain areas were observed to be blank (Figure 5C), the majority of the plate surface was confluent with green (live) cells. Similar cytotoxicity was associated with 3% v/v Ve in media, with the surface colonized by predominantly with live cells (Figure 5D) and a cell viability of ~50% (Figure 5H), which also should be considered as minimal. It is believed that blank areas, represent primarily cell detachment in PEG media (Figure 5C), as PEG is known for promoting poor cell adhesion, but primarily cell death in Ve media (Figure 5D), due to physical diffusion barrier of Ve oil floating on top of the wells preventing proper nutrient and oxygen exchange. Considering the concentration of PEG and Ve in physiological conditions would be significantly lower than the tested doses as they slowly diffuse out of the hydrogels upon hydration, cell cytotoxicity caused by these two components can be assumed to be minimal. In comparison, cell viability after treatment with PEGMA-co-Ve polymers of different molecular weights was above 40% in all cases (Figure 5E–G, and Figure 5H). In particular, PEGMA-co-Ve #50 showed the least cytotoxicity to fibroblasts (cell viability ~80%, Figure 5H). Consistent observations were noted in the live/dead stain; the cells were denser in PEGMA-co-Ve #50 treated media (Figure 5F), compared with PEGMA-co-Ve #20 (cell viability ~40%, Figure 5E) and #100 (cell viability ~40%, Figure 5G). It is speculated that higher molecular weight polymers are less likely to transport into cells and thus present lower cytotoxicities even at these high concentrations tested, with the higher apparent toxicity of #100 likely attributable not to inherent toxicity but rather the high viscosity of this formulation that can inhibit effective nutrient and oxygen exchange.[59] Because PEGMA-coVe #50 demonstrated satisfactory performance on cell proliferation and flowability with Ve, this polymer was selected for further in vivo study.

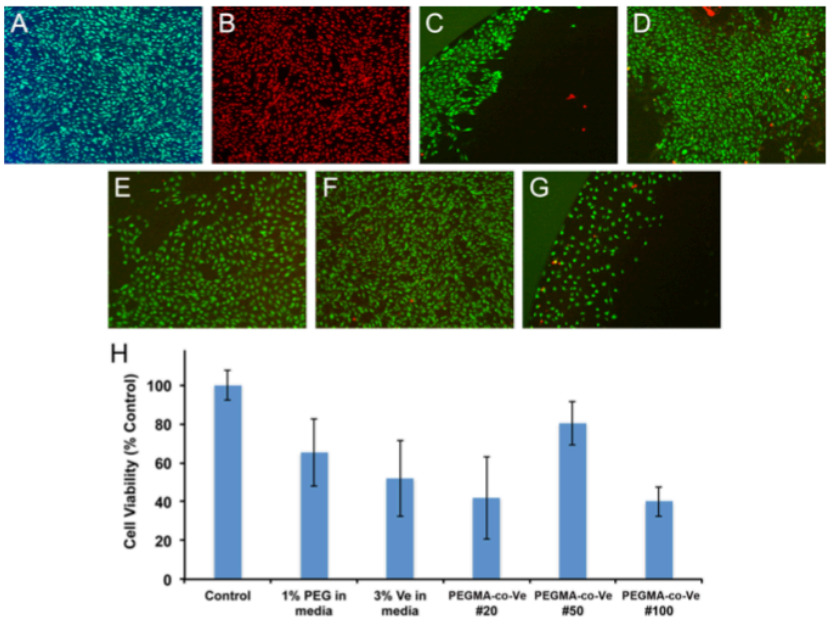

Figure 5. Fluorescence images of murine 3T3 fibroblast cells stained with the live/dead cytotoxicity assay kit (live cells: green; dead cells: red): (A and B) cell controls for (A) control cells stained after culture and (B) control cells killed after culture and stained. (C–G) Cells grown in media with (C) PEG (M_w = 300 Da, 1% v/v), (D) Ve (3% v/v), (E–G) PEGMA-*co*-Ve polymer with molecular weights of (E) M_w ~ 32 kDa, (F) M_w ~ 54 kDa, and (G): M_w ~ 60 kDa); (H) MTT assay results showing the viability of the cells cultured with all the components used in hydrogel relative to cell-only controls.

In Vivo Biocompatibility of PEGMA-co-Ve Gel in Eye and Skin Tissue. Any bioengineered material implanted into a host will elicit some immune response. For most conceivable applications, it is critical that this response is as benign as possible, with minimal inflammation and an eventual cessation of any foreign body response.[60] Ve has the potential to not only serve as hydrophobic gelling agent and drug solvent in these materials, but may also play other roles such as a free radical scavenger an anti-inflammatory, and/or an antithrombotic that might greatly enhance its potential as a biomaterial.[42–44]

In vivo evaluation was first performed in rat eyes. This choice was made for two reasons: (1) due to the transparency of the rat eye, it was possible to observe the gelation process in body tissue and (2) the injectable nature of these materials may find particular applicability in ophthalmics, in which extremely delicate and difficult to access tissues requires the use of minimally invasive surgical techniques. As shown in Figure 6A, a white gel with a clear boundary was formed in situ after injection. The gelation time in vitreous, similar to the discussion above in water, varied from almost immediately to a longer period depending on the formulation (Figure S9, Supporting Information). After ~2 h, the rats were sacrificed to look at the immediate physiological reactions upon the injection of hydrogel. The rat has a large lens, and the vitreous could be observed around the lens, presenting a line-like texture (Figure 6B-a). With the injection of Ve, the texture of vitreous was disrupted due to the immiscibility of Ve (Figure 6B-b). Following gel injection, the phase boundary between $50P_{42\%}PEG_{29\%}Ve_{29\%}$ gel and vitreous could be clearly observed (Figure 6B-c). Comparing these three eyes, the Ve and PEGMA-co-Ve

hydrogel demonstrated no retinal toxicity based on the lack of retinal necrosis, infiltration of inflammatory cells and morphological changes observed.

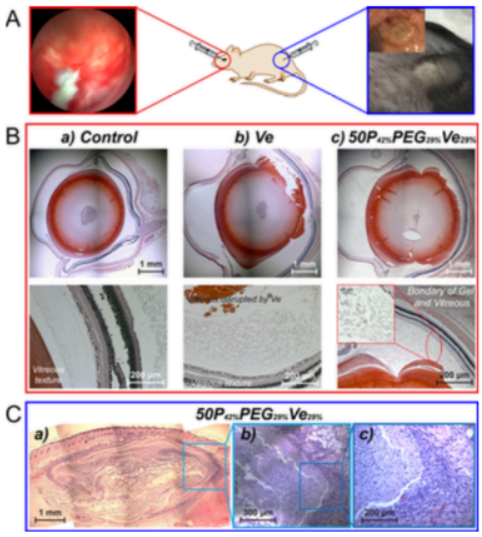

Figure 6. Histology of retinal and subcutaneous of sections: (A) Injection into rat eyes using a #30 gauge needle (examined with slit lamp microcopy, highlighted in red), and subcutaneous injection to mice using a #25 gauge needle (picture of tissue taken right after surgery, highlighted in blue). (B) Histology of retinal section of rat's eye following (a) saline control (continuous line-like texture could be observed after zoom-in, bottom picture), (b) Ve (line-like textures were disrupted and some discontinuous "islands", appear, bottom picture), and (c) $50P_{42\%}PEG_{29\%}Ve_{29\%}$ injections (boundary of gel and vitreous was indicated by red arrows, bottom picture). (C) Histology of hydrogels injected subcutaneously after 14 days.

In order to study the physiological reactions of PEGMA-coVe in vivo, such as long-term inflammatory responses and gel degradation, the gel was injected under the skin of mice for 15 days. Tissues were explanted, embedded in paraffin wax, sectioned, and stained with H&E to observe the local immune response. Consistent with the properties of a hydrogel, the boundary between the implant and host had become indistinct by this time point. The implant was nevertheless obvious, delineated by a thin oval fibrotic capsule (Figure 6C-a). While there was some immune response to the presence of the implant, it consisted mostly of infiltrating lymphocytes, and was, for the most part, extremely mild. Zoomed-in sections (Figure 6C-b,c) show the most immunologically active area. While this area appears somewhat granulomatous, there is no evidence of foreign body giant cells, necrosis, or neovascularisation, indicating a low-level tissue response.

Injectable hydrogels represent an extremely effective way to deliver drugs, cells, or genes to target tissues. Materials for use in vivo must be biocompatible and ideally should be biodegradable, with controllable gelation and hydration kinetics also highly desirable. The vitamin E-based polymer developed herein uses the presence of water to induce the gelation process, enabling both gelation and hydration rate control as a function of polymer structure while avoiding the need for less consistent environmental stimuli (e.g., local pH gradients that may cause inconsistency in gelation times and extent of gelation

in pH-driven gelling strategies) and/or potentially nonbioorthogonal chemistries to induce gelation. Relative to other existing materials, in situ gelation can be driven by mixing of a simple copolymer (prepared in a single polymerization step) dissolved in generally recognized as safe (GRAS) solvents, without the need for advanced organic synthesis steps or more advanced delivery strategies (e.g., double barrel syringes, which are particularly limiting in the very small volume injections required for ophthalmic applications). Given that the cell compatibility and in vivo tolerability tests performed collectively suggest acceptable properties for the use of these aqueous-driven gelation hydrogels in a biomedical context, there is potential to leverage this unique gelation strategy to develop injectable hydrogels relevant to a range of potential biomedical applications.

CONCLUSION

In this paper, we demonstrated the synthesis of a simple injectable hydrogel based on a one-step free radical polymerization of methacrylated poly(ethylene glycol) (PEG) and vitamin E (Ve). By dissolving the resulting copolymers in a solvent consisting of low molecular weight PEG and Ve and injecting the precursor polymers into an aqueous environment, hydrogels can be formed with controllable kinetics (from a few seconds to a few hours) upon exposure to an aqueous environment. The water content, mechanical strength (from a few pascals to a few kilopascals in compression), and drug release kinetics can be tuned simply by formulating PEGMA-coVe with different solvent combinations and concentrations and/or by varying the molecular weight of the polymers. Furthermore, in vitro live–dead and MTT assays and histological examination following in vivo injection into the vitreous and under the skin showed no significant toxicity to either cells or tissue over either the short-term or longer time periods. As such, PEGMA-co-Ve polymer has potential to be used not only as an injectable hydrogel, but also as an alternative for TPGS for nasal, pulmonary, ophthalmic, parenteral, or dermal delivery.

Associated content

Supporting Information:

The Supporting Information is available free of charge on the ACS Publications website at DOI: 10.1021/acs.biomac.6b01148.

Illustration of dialysis device for drug release; NMR spectra for PEGMA monomer, vitamin E, methacrylated Ve, and PEGMA-co-Ve copolymer with different molecular weight and block ratio; compression test of hydrogels; decomposition and degradation of hydrogels; particle size distribution of fragmented hydrogels; microscopic image of rat's eye injected with Ve and different hydrogels (PDF)

Injection video performed on a rat's eye (AVI)

Corresponding Author

*E-mail: sheardow@mcmaster.ca.

Notes

The authors declare no competing financial interest.

ACKNOWLEDGEMENTS

We thank Hamilton Health Sciences through the Boris Family Foundation, and the Natural Sciences and Engineering Research Council of Canada for financial support. We thank Dr. Rambarran for help with NMR characterization.

REFERENCES

(1)Kopeček,J.Hydrogelbiomaterials:Asmartfuture?Biomaterials 2007, 28 (34), 5185–5192.

(2) Van Vlierberghe, S.; Dubruel, P.; Schacht, E. Biopolymer-Based Hydrogels As Scaffolds for Tissue Engineering Applications: A Review. Biomacromolecules 2011, 12 (5), 1387–1408.

(3) Annabi, N.; Tamayol, A.; Uquillas, J. A.; Akbari, M.; Bertassoni, L. E.; Cha, C.; Camci-Unal, G.; Dokmeci, M. R.; Peppas, N. A.; Khademhosseini, A. 25th Anniversary Article: Rational Design and Applications of Hydrogels in Regenerative Medicine. Adv. Mater. 2014, 26 (1), 85–124.

(4) Choi, B.; Loh, X. J.; Tan, A.; Loh, C. K.; Ye, E.; Joo, M. K.; Jeong, B. Introduction to In Situ Forming Hydrogels for Biomedical Applications. In In-Situ Gelling Polymers: For Biomedical Applications; Loh, J. X., Ed.; Springer Singapore: Singapore, 2015; pp 5–35.

(5) Tan, H.; Marra, K. G. Injectable, Biodegradable Hydrogels for Tissue Engineering Applications. Materials 2010, 3 (3), 1746.

(6) Li, Y.; Rodrigues, J.; Tomas, H. Injectable and biodegradable hydrogels: gelation, biodegradation and biomedical applications. Chem. Soc. Rev. 2012, 41 (6), 2193–2221.

(7) Sivashanmugam, A.; Arun Kumar, R.; Vishnu Priya, M.; Nair, S. V.; Jayakumar, R. An overview of injectable polymeric hydrogels for tissue engineering. Eur. Polym. J. 2015, 72, 543–565.

(8) Bakaic, E.; Smeets, N. M. B.; Hoare, T. Injectable hydrogels based on poly(ethylene glycol) and derivatives as functional biomaterials. RSC Adv. 2015, 5 (45), 35469–35486.

(9) Pakulska, M. M.; Vulic, K.; Tam, R. Y.; Shoichet, M. S. Hybrid Crosslinked Methylcellulose Hydrogel: A Predictable and Tunable Platform for Local Drug Delivery. Adv. Mater. 2015, 27 (34), 5002– 5008.

(10) Kharkar, P. M.; Rehmann, M. S.; Skeens, K. M.; Maverakis, E.; Kloxin, A. M. Thiol–ene Click Hydrogels for Therapeutic Delivery. ACS Biomater. Sci. Eng. 2016, 2 (2), 165–179.

(11) Patenaude, M.; Hoare, T. Injectable, Mixed Natural-Synthetic Polymer Hydrogels with Modular Properties. Biomacromolecules 2012, 13 (2), 369–378.

(12) Grover, G. N.; Lam, J.; Nguyen, T. H.; Segura, T.; Maynard, H. D. Biocompatible Hydrogels by Oxime Click Chemistry. Biomacromolecules 2012, 13 (10), 3013–3017.

(13) Choh, S.-Y.; Cross, D.; Wang, C. Facile Synthesis and Characterization of Disulfide-Cross-Linked Hyaluronic Acid Hydrogels for Protein Delivery and Cell Encapsulation. Biomacromolecules 2011, 12 (4), 1126–1136.

(14) Jin, R.; Moreira Teixeira, L. S.; Krouwels, A.; Dijkstra, P. J.; van Blitterswijk, C. A.; Karperien, M.; Feijen, J. Synthesis and characterization of hyaluronic acid–poly(ethylene glycol) hydrogels via Michael addition: An injectable biomaterial for cartilage repair. Acta Biomater. 2010, 6 (6), 1968–1977.

(15) Kharkar, P. M.; Kiick, K. L.; Kloxin, A. M. Design of thioland light-sensitive degradable hydrogels using Michael-type addition reactions. Polym. Chem. 2015, 6 (31), 5565–5574.

(16) Yu, Y.; Deng, C.; Meng, F.; Shi, Q.; Feijen, J.; Zhong, Z. Novel injectable biodegradable glycol chitosan-based hydrogels crosslinked by Michael-type addition reaction with oligo(acryloyl carbonate)-bpoly(ethylene glycol)-b-oligo(acryloyl carbonate) copolymers. J. Biomed. Mater. Res., Part A 2011, 99A (2), 316–326.

(17) Chou, A. I.; Akintoye, S. O.; Nicoll, S. B. Photo-crosslinked alginate hydrogels support enhanced matrix accumulation by nucleus pulposus cells in vivo. Osteoarthritis and Cartilage 2009, 17 (10), 1377–1384.

(18) Tan, G.; Wang, Y.; Li, J.; Zhang, S. Synthesis and Characterization of Injectable Photocrosslinking Poly (ethylene glycol) Diacrylate based Hydrogels. Polym. Bull. 2008, 61 (1), 91–98.

(19) Lee, S.-Y.; Tae, G. Formulation and in vitro characterization of an in situ gelable, photo-polymerizable Pluronic hydrogel suitable for injection. J. Controlled Release 2007, 119 (3), 313–319.

(20) Balakrishnan, B.; Jayakrishnan, A. Self-cross-linking biopolymers as injectable in situ forming biodegradable scaffolds. Biomaterials 2005, 26 (18), 3941–3951.

(21) Jin, R.; Moreira Teixeira, L. S.; Dijkstra, P. J.; van Blitterswijk, C. A.; Karperien, M.; Feijen, J. Enzymatically-crosslinked injectable hydrogels based on biomimetic dextran–hyaluronic acid conjugates for cartilage tissue engineering. Biomaterials 2010, 31 (11), 3103– 3113.

(22) Jin, R.; Hiemstra, C.; Zhong, Z.; Feijen, J. Enzyme-mediated fast in situ formation of hydrogels from dextran–tyramine conjugates. Biomaterials 2007, 28 (18), 2791–2800.

(23) Baskin, J. M.; Bertozzi, C. R. Bioorthogonal Click Chemistry: Covalent Labeling in Living Systems. QSAR Comb. Sci. 2007, 26 (11– 12), 1211–1219.

(24) Boffito, M.; Sirianni, P.; Di Rienzo, A. M.; Chiono, V. Thermosensitive block copolymer hydrogels based on poly(εcaprolactone) and polyethylene glycol for biomedical applications: State of the art and future perspectives. J. Biomed. Mater. Res., Part A 2015, 103 (3), 1276–1290.

(25) Payyappilly, S.; Dhara, S.; Chattopadhyay, S. Thermoresponsive biodegradablePEG-PCL-PEGbasedinjectablehydrogelforpulsatile insulin delivery. J. Biomed. Mater. Res., Part A 2014, 102 (5), 1500– 1509.

(26) Kim, S. Y.; Lee, S. C. Thermo-responsive injectable hydrogel system based on poly(N-isopropylacrylamide-co-vinylphosphonic

acid). I. Biomineralization and protein delivery. J. Appl. Polym. Sci. 2009, 113 (6), 3460–3469.

(27) Klouda, L.; Mikos, A. G. Thermoresponsive hydrogels in biomedical applications. Eur. J. Pharm. Biopharm. 2008, 68 (1), 34–45. (28) He, C.; Kim, S. W.; Lee, D. S. In situ gelling stimuli-sensitive block copolymer hydrogels for drug delivery. J. Controlled Release

2008, 127 (3), 189–207.

(29) Shim, W. S.; Kim, J.-H.; Kim, K.; Kim, Y.-S.; Park, R.-W.; Kim,

I.-S.; Kwon, I. C.; Lee, D. S. pHand temperature-sensitive, injectable, biodegradable block copolymer hydrogels as carriers for paclitaxel. Int. J. Pharm. 2007, 331 (1), 11–18.

(30) Shim, W. S.; Yoo, J. S.; Bae, Y. H.; Lee, D. S. Novel Injectable pH and Temperature Sensitive Block Copolymer Hydrogel. Biomacromolecules 2005, 6 (6), 2930–2934.

(31) Lee, A. L. Z.; Ng, V. W. L.; Gao, S.; Hedrick, J. L.; Yang, Y. Y. Injectable Biodegradable Hydrogels from Vitamin D-Functionalized Polycarbonates for the Delivery of Avastin with Enhanced Therapeutic Efficiency against Metastatic Colorectal Cancer. Biomacromolecules 2015, 16 (2), 465–475.

(32) Lee, A. L. Z.; Ng, V. W. L.; Gao, S.; Hedrick, J. L.; Yang, Y. Y. Injectable Hydrogels from Triblock Copolymers of Vitamin EFunctionalized Polycarbonate and Poly(ethylene glycol) for Subcutaneous Delivery of Antibodies for Cancer Therapy. Adv. Funct. Mater. 2014, 24 (11), 1538–1550.

(33) Wu, Y.; Guo, B.; Ma, P. X. Injectable Electroactive Hydrogels Formed via Host–Guest Interactions. ACS Macro Lett. 2014, 3 (11), 1145–1150.

(34) Hoare, T. R.; Kohane, D. S. Hydrogels in drug delivery: Progress and challenges. Polymer 2008, 49 (8), 1993–2007.

(35) Patenaude, M.; Hoare, T. Injectable, Degradable Thermoresponsive Poly(N-isopropylacrylamide) Hydrogels. ACS Macro Lett. 2012, 1 (3), 409–413.

(36) Kamata, H.; Kushiro, K.; Takai, M.; Chung, U.-i.; Sakai, T. NonOsmotic Hydrogels: A Rational Strategy for Safely Degradable Hydrogels. Angew. Chem., Int. Ed. 2016, 55, 9282.

(37) Aamer, K. A.; Sardinha, H.; Bhatia, S. R.; Tew, G. N. Rheological studies of PLLA–PEO–PLLA triblock copolymer hydrogels. Biomaterials 2004, 25 (6), 1087–1093.

(38) Chan, Y. P.; Meyrueix, R.; Kravtzoff, R.; Nicolas, F.; Lundstrom, K. Review on Medusa®:a polymer-based sustained release technology for protein and peptide drugs. Expert Opin. Drug Delivery 2007, 4 (4), 441–451.

(39)Almeida,H.;Amaral,M.H.;Lobaõ,P.;Silva,A.C.;Loboa,J.M. S. Applications of polymeric and lipid nanoparticles in ophthalmic pharmaceutical formulations: present and future considerations. J. Pharm. Pharm. Sci. 2014, 17 (3), 278–293.

(40) Wang, R.; Hughes, T.; Beck, S.; Vakil, S.; Li, S.; Pantano, P.; Draper, R. K. Generation of toxic degradation products by sonication of Pluronic® dispersants: implications for nanotoxicity testing. Nanotoxicology 2012, 7 (7), 1272–1281.

(41) Jokerst, J. V.; Lobovkina, T.; Zare, R. N.; Gambhir, S. S. Nanoparticle PEGylation for imaging and therapy. Nanomedicine 2011, 6 (4), 715–728.

(42) Azzi, A.; Ricciarelli, R.; Zingg, J.-M. Non-antioxidant molecular functions of α-tocopherol (vitamin E). FEBS Lett. 2002, 519 (1–3), 8–10.

(43) Constantinides, P. P.; Han, J.; Davis, S. S. Advances in the Use of Tocols as Drug Delivery Vehicles. Pharm. Res. 2006, 23 (2), 243– 255.

(44) Frank, J. Beyond vitamin E supplementation: An alternative strategy to improve vitamin E status. J. Plant Physiol. 2005, 162 (7), 834–843.

(45)Duhem,N.;Danhier,F.;Preát,V.VitaminE-basednanomedicines for anti-cancer drug delivery. J. Controlled Release 2014, 182, 33–44.

(46) Zhang, Z.; Tan, S.; Feng, S.-S. Vitamin E TPGS as a molecular biomaterial for drug delivery. Biomaterials 2012, 33 (19), 4889–4906.

(47) Guo, Y.; Luo, J.; Tan, S.; Otieno, B. O.; Zhang, Z. The applications of Vitamin E TPGS in drug delivery. Eur. J. Pharm. Sci. 2013, 49 (2), 175–186.

(48) Kwon, O. H.; Kikuchi, A.; Yamato, M.; Sakurai, Y.; Okano, T. Rapid cell sheet detachment from Poly(N-isopropylacrylamide)grafted porous cell culture membranes. J. Biomed. Mater. Res. 2000, 50 (1), 82–89.

(49) Chen, J.; Park, K. Synthesis and characterization of superporous hydrogel composites. J. Controlled Release 2000, 65 (1–2), 73–82.

(50) Reis, A. V.; Guilherme, M. R.; Cavalcanti, O. A.; Rubira, A. F.; Muniz, E. C. Synthesis and characterization of pH-responsive hydrogels based on chemically modified Arabic gum polysaccharide. Polymer 2006, 47 (6), 2023–2029.

(51) Chang, C.; Duan, B.; Zhang, L. Fabrication and characterization of novel macroporous cellulose–alginate hydrogels. Polymer 2009, 50 (23), 5467–5473.

(52) Gunn, J. W.; Turner, S. D.; Mann, B. K. Adhesive and mechanical properties of hydrogels influence neurite extension. J. Biomed. Mater. Res. 2005, 72A (1), 91–97.

(53) Slaughter, B. V.; Khurshid, S. S.; Fisher, O. Z.; Khademhosseini, A.; Peppas, N. A. Hydrogels in Regenerative Medicine. Adv. Mater. 2009, 21 (32–33), 3307–3329.

(54) Nguyen, K. T.; West, J. L. Photopolymerizable hydrogels for tissue engineering applications. Biomaterials 2002, 23 (22), 4307– 4314.

(55) Torffvit, O.; Rippe, B. Size and Charge Selectivity of the Glomerular Filter in Patients with Insulin-Dependent Diabetes mellitus: Urinary Immunoglobulins and Glycosaminoglycans. Nephron 1999, 83 (4), 301–307.

(56) Yamaoka, T.; Tabata, Y.; Ikada, Y. Distribution and tissue uptake of poly(ethylene glycol) with different molecular weights after intravenous administration to mice. J. Pharm. Sci. 1994, 83 (4), 601–606.

(57) Folmer, B. M.; Barron, D.; Hughes, E.; Miguet, L.; Sanchez, B.; Heudi, O.; Rouvet, M.; Sagalowicz, L.; Callier, P.; Michel, M.; Williamson, G. Monocomponent hexaand dodecaethylene glycol succinyl-tocopherol esters: Self-assembly structures, cellular uptake and sensitivity to enzyme hydrolysis. Biochem. Pharmacol. 2009, 78 (12), 1464–1474.

(58) Sung, J. H.; Shuler, M. L. A micro cell culture analog ([small micro]CCA) with 3-D hydrogel culture of multiple cell lines to assess metabolism-dependent cytotoxicity of anti-cancer drugs. Lab Chip 2009, 9 (10), 1385–1394.

(59) Duhem, N.; Rolland, J.; Riva, R.; Guillet, P.; Schumers, J.-M.; Jeŕome, C.; Gohy, J.-F.; Preát, V. Tocol modified glycol chitosan for the oral delivery of poorly soluble drugs. Int. J. Pharm. 2012, 423 (2), 452–460.

(60) Říhova,´ B. Immunocompatibility and biocompatibility of cell delivery systems. Adv. Drug Delivery Rev. 2000, 42 (1–2), 65–80.